

Surface diffusion in the low-friction limit: Occurrence of long jumps

L. Y. Chen

Division of Earth and Physical Sciences, University of Texas at San Antonio, San Antonio, Texas 78249

M. R. Baldan

*I.N.P.E., 12201-970, São José Dos Campos, São Paulo, Brazil
and Faculdade de Engenharia, Universidade São Francisco, Itatiba, São Paulo, Brazil*

S. C. Ying

Department of Physics, Brown University, Providence, Rhode Island 02912

(Received 26 February 1996)

We present a molecular dynamics (MD) study of a Brownian particle in a two-dimensional periodic potential. For a separable potential, the study of the diffusion constant along the symmetry directions reduces to two one-dimensional problems. In this case, our MD study agrees with the existing analytical results on the temperature and the friction (η) dependence of the diffusion constant (D). For a nonseparable and anisotropic potential such as the adsorption potential on a bcc(110) surface, the present study predicts an alternative $D \sim 1/\eta^{0.5}$ dependence in the low friction regime as opposed to the $D \sim 1/\eta$ dependence found in previous studies of one-dimensional or separable potentials. We find that the dependence of D on η in the low friction regime is directly related to the occurrence of long jumps. The probability for the long jumps depends not only sensitively on the value of the friction but also on the geometry of the surface. On the bcc(110) surface, the path connecting adjoining adsorption sites does not coincide with the direction of easy crossing at the saddle point. Consequently, the probability of deactivation is enhanced, leading to the reduction of long jumps and the different dependence of D on η . [S0163-1829(96)09035-2]

A variety of phenomena in physics and other fields can be modeled as Brownian motion in an external potential.^{1,2} One particular example is the diffusion of adsorbed atoms (adatoms) on solid surfaces.³ In this case, the problem can be described by a Langevin equation for the adatom, or, equivalently, a Fokker-Planck equation for the distribution function in the phase space. For the one-dimensional (1D) system, analytical solutions have been achieved for the Langevin equation or the equivalent Fokker-Planck equation.⁴⁻⁹ However, an analytical solution of the 2D Langevin equation, particularly in the low friction regime, poses a considerable challenge. It has only been accomplished in the special case of separable potentials containing no cross terms depending on both Cartesian components of the adatom displacement vector.⁸ In this paper, we present a molecular dynamics (MD) solution of the Langevin equation describing the Brownian motion of an adatom in an arbitrary 2D adsorption potential. This method is particularly well suited for the low friction regime, thus making it complementary to the matrix continued-fraction-expansion approach^{5,6,8} which works well in the high to intermediate friction regime. We will show below that in the low friction regime, the variation of the diffusion rate with the friction parameter η depends crucially on the details of the adsorption potential, and the result derived for 1D or the special 2D separable potentials is not applicable to the case of arbitrary non-separable 2D potentials.

We first consider the qualitative features of the Brownian motion of the adatom. At high temperatures, the effect of the periodic adsorption potential is negligible and the motion reduces to the case of free Brownian particle in a viscous

fluid. As the temperature is lowered, there is a crossover to the thermal activated behavior. In this low temperature regime, diffusion proceeds by uncorrelated jumps over the barrier from one adsorption potential well to another, and the temperature dependence of the diffusion constant obeys the well known Arrhenius form, with the diffusion barrier determined by the difference in the value of the adsorption potential between the saddle point (2D) or the barrier (1D) and the well. The prefactor in front of the exponential, however, contains the real dynamical information. In general, it depends on the value of the friction which characterizes the strength of the coupling to the substrate excitations. In the high friction regime, D decreases with friction η as $D \sim \eta^{-1}$. This behavior follows from the fact that the probability for the particle to recross a barrier increases with increasing value of the friction. For intermediate values of friction, the transition state theory (TST) is approximately valid and the prefactor is then determined entirely by equilibrium quantities and does not depend on the friction. In the low friction regime, the activation rate of escaping from the well decreases with decreasing value of the friction.⁴ However, the deactivation rate also decreases with η , which implies a larger probability of long jumps. In fact, it has been shown that for a 1D or a 2D separable potential system, the activation rate goes as $\sim \eta$, while the mean square jumping displacement behaves as $\sim 1/\eta^2$ in the limit $\eta \rightarrow 0$. This then leads to the dependence of the diffusion constant on the friction in the form $D \sim 1/\eta$.^{5,8} The occurrence of these long jumps in the low temperature regime has been observed in previous MD simulations as well as in a number of experiments designed to measure surface diffusion.^{10,11} We expect now that for a gen-

eral 2D potential, most of these qualitative considerations would still hold true with one noticeable exception. While the activation rate and the recrossing rate depends only on the local properties near the minimum and the barrier, the deactivation rate and hence the probability of the long jumps should depend sensitively on the global geometry of the surface. This could be seen from the following considerations. The adatom crosses the saddle point along the direction of the steepest descent. For a general 2D adsorption potential, this does not coincide with the direction joining two adjacent minima of the adsorption potential. The adatom would then have to bounce around in the next adsorption well before acquiring the right direction for the next crossing. This required change of direction obviously enhances the deactivation rate and lowers the probability of long jumps relative to the 1D or 2D separable potential. Similar effects originating from the nonseparability of the normal and in-plane motion have been noted by several authors.^{12,13} The effect also should be strongly dependent on the geometry of the surface. Thus, the primary focus of the present MD study concerns the diffusion anisotropy and the dependence of the long jumps on the friction in a nonseparable 2D potential. In what follows, we first describe the formulation of our MD simulation. Then we compare numerical results for a 2D system of separable adsorption potential with known analytic results as a check of the accuracy of our numerical procedures. The main body of our results are obtained for a 2D nonseparable potential having the symmetry of a bcc(110) surface. For this system, we present numerical results of diffusion constants along two principal axes for various temperatures and a range of friction values. To illustrate the sensitive dependence of long jumps on the surface geometry, we present data for probability vs jump displacements, activation rate vs friction, and mean square jump displacements vs friction.

Consider an adatom diffusing in a 2D periodic potential $U(x,y)$. The adatom's coupling to the substrate excitations is characterized by a constant friction η . We assume that the time scale for the substrate excitations is much shorter than that for the adatom so that memory effects can be neglected. We describe the motion of the adatom in terms of the Langevin equation,

$$m\ddot{x}(t) = -\partial_x U(x,y) - \eta\dot{x} + \xi_x(t), \quad (1)$$

$$m\ddot{y}(t) = -\partial_y U(x,y) - \eta\dot{y} + \xi_y(t), \quad (2)$$

where m is the particle's mass and x and y , the displacements. The Gaussian white noises, ξ_x and ξ_y , have zero mean and the following correlations:

$$\langle \xi_{x(y)}(t)\xi_{x(y)}(t') \rangle = k_B T \eta \delta(t-t'), \quad \langle \xi_x(t)\xi_y(t') \rangle = 0, \quad (3)$$

with k_B the Boltzmann constant and T the temperature. The diffusion constants along the x and y axes are related to the mean square displacements as

$$D_x = \left. \frac{\langle x^2(t) \rangle}{2t} \right|_{t \rightarrow \infty}, \quad D_y = \left. \frac{\langle y^2(t) \rangle}{2t} \right|_{t \rightarrow \infty}. \quad (4)$$

Equivalently, they can be expressed in terms of the Laplace transform of the velocity-velocity correlation function,

$$D_x = \int_0^\tau dt \langle v_x(t)v_x(0) \rangle_{\tau \rightarrow \infty},$$

$$D_y = \int_0^\tau dt \langle v_y(t)v_y(0) \rangle_{\tau \rightarrow \infty}. \quad (5)$$

In the above equations, the thermal statistical average $\langle \rangle$ means average over the initial conditions and over the stochastic paths obtained by numerically integrating the Langevin equations (1) and (2).

Considering that the deterministic forces $\partial_x U$ and $\partial_y U$ remain approximately constant in a short time interval $(t, t+dt)$, the Langevin equations (1) and (2) can be integrated with the random forces treated exactly. Then the algorithm can be written as¹⁴

$$x(t+dt) = x(t) + c_1 dt v_x(t) + c_2 dt^2 a_x(t) + \delta x^G, \quad (6)$$

$$y(t+dt) = y(t) + c_1 dt v_y(t) + c_2 dt^2 a_y(t) + \delta y^G, \quad (7)$$

$$v_x(t+dt) = c_0 v_x(t) + c_1 dt a_x(t) + \delta v_x^G, \quad (8)$$

$$v_y(t+dt) = c_0 v_y(t) + c_1 dt a_y(t) + \delta v_y^G, \quad (9)$$

where

$$c_0 = e^{-\eta dt}, \quad c_1 = (1 - c_0)/\eta dt, \quad c_2 = (1 - c_1)/\eta dt. \quad (10)$$

$\delta x^G, \delta y^G$ and $\delta v_x^G, \delta v_y^G$ are, respectively, the displacements and velocity components caused by the random forces ξ_x, ξ_y . δx^G and δv_x^G are Gaussian and correlated, with variance matrix elements,

$$\langle \delta x^G \delta x^G \rangle = dt^2 \frac{k_B T}{m} [2 - (3 - 4c_0 + c_0^2)/\eta dt]/\eta dt, \quad (11)$$

$$\langle \delta v_x^G \delta v_x^G \rangle = \frac{k_B T}{m} (1 - c_0^2), \quad (12)$$

$$\langle \delta x^G \delta v_x^G \rangle = dt \frac{k_B T}{m} (1 - c_0)^2 / \eta dt. \quad (13)$$

An identical form of variance matrix holds for the correlated Gaussian variables δy^G and δv_y^G .

We first verify the accuracy of our MD simulation approach by performing calculations for the separable potential

$$U(x,y) = V_0 \left[2 - \cos\left(\frac{2\pi x}{a}\right) - \cos\left(\frac{2\pi y}{a}\right) \right], \quad (14)$$

where a is the lattice constant. The diffusion barrier for this potential Δ equals $2V_0$ and the bare frequencies of the two frustrated translational modes ω_x and ω_y both are equal to $\omega_0 \equiv 2\pi/a\sqrt{V_0/m}$. In this case, the motion along the x direction is separable from the y direction as is visible from curvature lines of $U(x,y)$ illustrated in Fig. 1. Our MD simulation for this potential recovers the results of previous studies using the matrix continued fraction expansion method.^{5,8} At low temperatures, diffusion proceeds by thermally activated jumps across the saddle points. The temperature dependence of the diffusion constant conforms to the Arrhenius

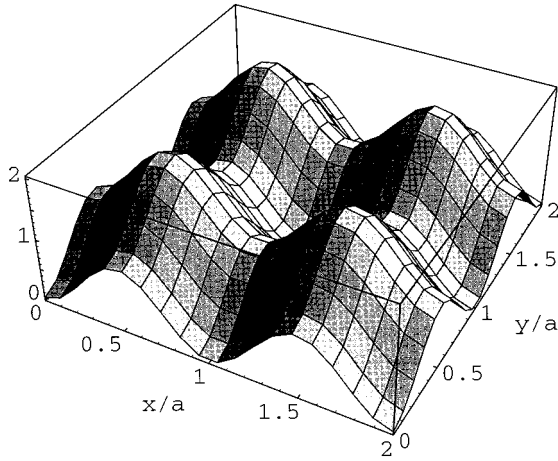


FIG. 1. A separable periodic potential $U(x,y)$. The potential is scaled by the diffusion barrier.

exponential form (Fig. 2). As discussed earlier, the dependence of the prefactor on the friction η divides into three regimes. At high friction values such that $\eta/\omega_0 \gg 1$, we have $D \sim 1/\eta$. At low friction value such that $\eta/\omega_0 \ll 1$, we also have the dependence $D \sim 1/\eta$. In the intermediate regime around the value of $\eta/\omega_0 \sim 1$, the prefactor varies more slowly as a function of friction compared with the other two regimes. The value of the diffusion constant in this regime is centered at the TST result $D = (\omega_0/2\pi)a^2 e^{-\Delta/k_B T}$. This is the regime where neither significant recrossing nor long jumps occur and where the error of TST is minimized.

We next consider a nonseparable potential of the symmetry that is appropriate for adsorption on a bcc(110) surface,

$$U(x,y) = V_0 \left[1 + \sin\left(\frac{2\pi x}{a}\right) \sin\left(\frac{2\pi y}{\sqrt{2}a}\right) \right], \quad (15)$$

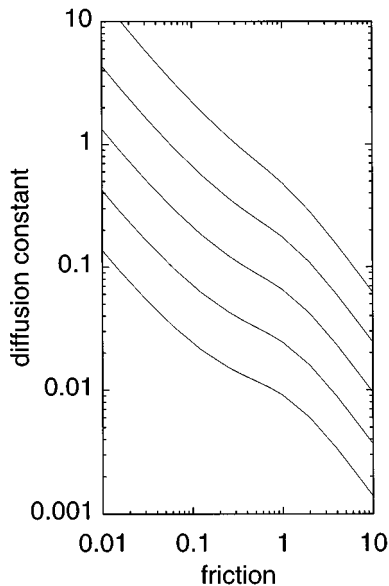


FIG. 2. Diffusion constant $D/\omega_0 a^2$ vs friction η/ω_0 for inverse temperature $\beta\Delta = 0.1$ (top), 0.3 (second), 4 (third), 5 (fourth), and 6 (bottom).

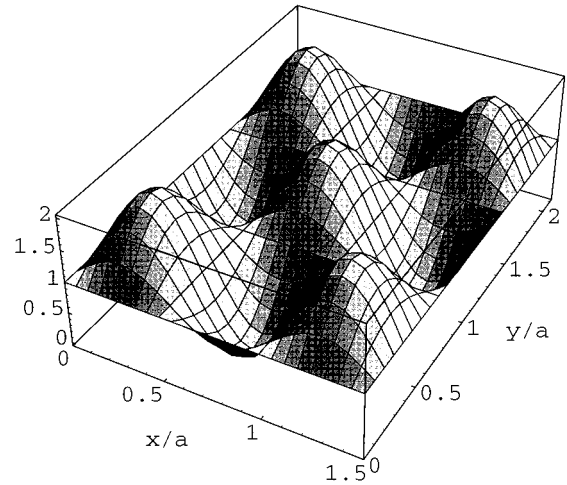


FIG. 3. A nonseparable periodic potential $U(x,y)$ of bcc(110) surface symmetry (scaled by the diffusion barrier).

where a is lattice constant. The x axis is along the (001) direction while y axis is along the (110) direction. This potential is illustrated in Fig. 3. The saddle points are located at $(x_S = ma/2, y_S = na/\sqrt{2})$ with arbitrary integers m, n . The potential wells are located at $[x_W = (m+1/2)a/2, y_W = (n-1/2)a/\sqrt{2}]$ and $[x_W = (m-1/2)a/2, y_W = (n+1/2)a/\sqrt{2}]$ while the maxima occur at $[x_M = (m+1/2)a/2, y_M = (n+1/2)a/\sqrt{2}]$ and $[x_M = (m-1/2)a/2, y_M = (n-1/2)a/\sqrt{2}]$. The diffusion barrier Δ for this potential is equal to V_0 and the bare frequencies of two frustrated translational modes have the frequencies $\omega_x = \omega_0$ and $\omega_y = \omega_0/2$, respectively. As is visible in Fig. 3, the principal axes of the curvature matrix of the potential at a saddle point are not aligned along the well-saddle point-well line or the maximum-saddle point-maximum line. For this nonseparable potential, our MD results for diffusion constants D_x and D_y vs temperature T and friction η are plotted in Fig. 4.

First, we examine the temperature dependence of the diffusion constant. At very high temperatures *s.t.* $k_B T \gg \Delta$, the effect of the periodic adsorption potential is negligible. The diffusion constant is isotropic and takes on the familiar form $D_x \approx D_y \approx k_B T / \eta$ which is characteristic of the motion of a free Brownian particle. At low temperatures *s.t.* $k_B T \ll \Delta$, the particle resides in a potential well for most of the time and diffusion is dominated by thermal activated crossing over the saddle points from one well to another. In this case, the ratio between the mean square displacements along the x and y axis is determined by the symmetry and equals 1/2. Consequently, at low temperatures the ratio of the the diffusion constants along the x and y directions reach asymptotically the geometrical ratio 1/2.

Next we consider the dependence of the diffusion constant D (which stands for D_x or D_y) on the friction η in the low temperature regime. Again, the dependence can be classified into three regimes in a manner similar to the case for the separable potential. The high friction $D \sim 1/\eta$ and the approximate TST behavior in the intermediate friction regime are parallel to those for the separable potential and have the same physical origins. In the low friction regime where $\eta/\omega_0 \ll 1$, we find a new behavior. Instead of the $D \sim 1/\eta$ dependence, our MD data in this regime indicates a friction

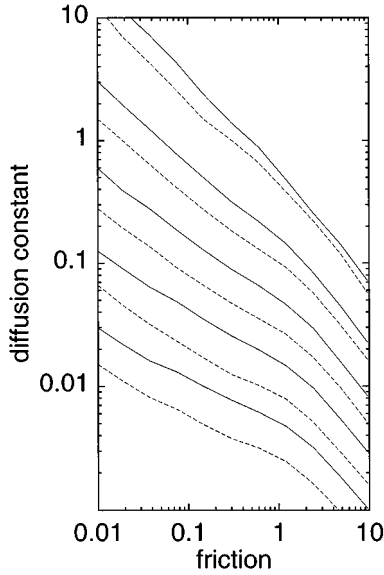


FIG. 4. Diffusion constants along principal axes, $D_x/\omega_0 a^2$ along (001) (dashed) and $D_y/\omega_0 a^2$ along $(\bar{1}\bar{1}0)$ (solid) vs friction η/ω_0 for temperatures $\Delta/k_B T = 1.3$ (top pair), 2.55 (second), 3.75 (third), 4.95 (fourth), and 6.15 (bottom).

dependence of the form $D \sim 1/\eta^{0.5}$. That is, the value of the diffusion constant increases more slowly as a function of decreasing value of the friction relative to that for the separable potential. This behavior stems from the nonalignment of the principal axes with the easiest diffusion path through saddle points. After crossing the saddle point along the path of the steepest descent, the adatom has to change direction in the new well region before finding its way to cross the next saddle point as illustrated, for example, in Fig. 5. This required change of direction between sequential crossings over saddle point enhances the probability of deactivation and equilibration of the adatom. Consequently, the probability of occurrence of long jumps is reduced relative to the situation of 1D or separable potential where no change of direction between sequential crossings of saddle point in a long jump is necessary. This ultimately leads to the weaker dependence

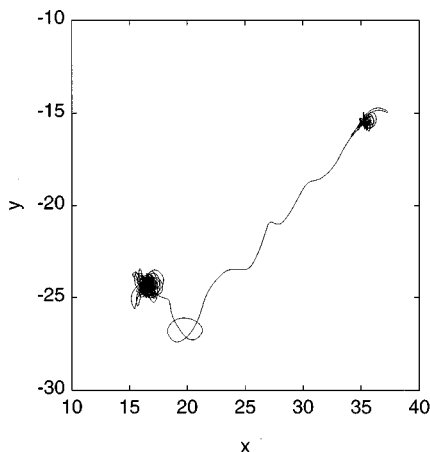


FIG. 5. A typical jump trajectory. $\Delta/k_B T = 6.15$ and $\eta/\omega_0 = 0.01875$.

$D \sim 1/\eta^{0.5}$ of the diffusion constant on the friction as observed in our MD simulations.

To demonstrate explicitly the picture presented in the last section. We examine in this section the probability of the occurrence of long jumps in the low friction regime. This is done via two separate approaches. The first is by direct examination of the trajectories generated in our stochastic dynamics simulations. To count the number of jump events from numerical trajectories, we need a criterion to identify the start and the end of a jump. Naturally, at low temperatures, a jump starts when the particle acquires an energy greater than the diffusion barrier Δ , and the end of the jump should be when the adatom loses its memory of the previous motion. The actual moment of the loss of memory is numerically hard to pinpoint exactly. We have identified it as the point when the energy of the adatom drops to a value of $3k_B T$ below the saddle point. The exact choice of this cutoff energy below which we identify the adatom to have suffered memory loss is somewhat arbitrary. In fact, the choice of $2k_B T$ as a cutoff in this case yields identical results for determining the jump events. We have also tried counting jump events with a velocity criterion. In this case, a jump event ends when the velocity component along $\langle \bar{1}\bar{1}1 \rangle$ or $\langle \bar{1}11 \rangle$ reverses its sign. This is less plausible as a link to the loss of memory compared with the energy criterion. The energy and the velocity criteria actually yield different values for the activation/deactivation rate and the mean square displacements of the jump events. However, when the diffusion constant is calculated as a product of the activation rate and the mean square displacements, the two criteria yield the same result.

Experimentally, long jumps have been observed either directly or deduced by comparison with a random walk theory involving jumps of different lengths. In the first category is the STM measurement by Ganz *et al.*¹⁰ The long jump in this experiment is defined based on the residence time in a well, namely, a jump is considered to have ended when the adatom stays in a well longer than some typical time τ comparable to the observation time and much longer than a vibrational period $1/\omega_0$. This definition of long jump does not necessarily coincide with that based on the loss of memory, although they are qualitatively similar. The second category of experiment compares physical observable quantity with the corresponding theoretical expression in a random walk model in which the adatom performs uncorrelated jumps of various lengths.^{11,15} For example, the quasielastic peak width in the dynamic structure factor is given in the random walk model by the expression¹⁶

$$\Gamma(\mathbf{K}) = 2\gamma \sum_{m,n} P(\mathbf{r}_{m,n}) [1 - \cos(\mathbf{K} \cdot \mathbf{r}_{m,n})]. \quad (16)$$

Here, γ is the total jump rate. Thus, $P(\mathbf{r}_{m,n})$ can be obtained by a back Fourier transform of the observed $\Gamma(\mathbf{K})$. Numerically, this provides yet another way of finding both the jump rate and the relative occurrence of jumps of different lengths. The procedure is first to evaluate the dynamical structure factor numerically and then subtract off a slowly varying background near the quasielastic peak. This background comes from vibrational contributions and is not included in the expression $\Gamma(\mathbf{K})$ discussed above. One can then evaluate

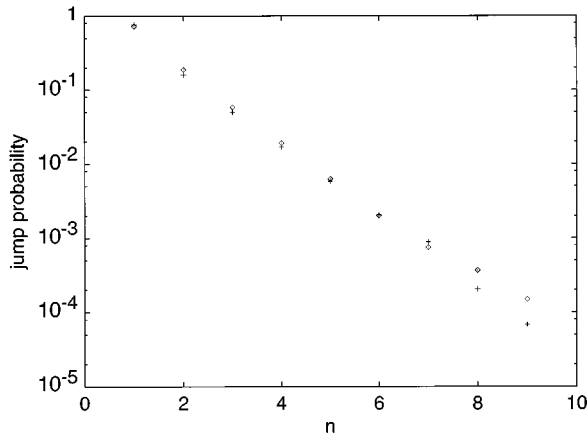


FIG. 6. Jump probability for the separable potential. The parameters are $\Delta/k_B T=3.9$ and $\eta=0.15\omega_0$. The diamonds are for data extracted from the dynamic structure factor and the crosses for that from direct counting of the molecular dynamics trajectory.

$\Gamma(\mathbf{K})$ as a function of \mathbf{K} and back Fourier transform to obtain $P(\mathbf{r}_{m,n})$. This provides an alternative way of studying the long jumps without the somewhat uncertain criterion of determining the end of a jump event. For the separable potential in Eq. (14), we have computed the probability $\sum_n P(\mathbf{r}_{m,n})$ vs m obtained by means of dynamic structure and by means of direct counting using the energy criterion. The results are plotted in Fig. 6. It is seen that the jump probabilities $P(\mathbf{r}_{m,n})$ [$\mathbf{r}_{m,n}=(ma,na,0)$] obtained by the two methods agree well with each other. For the nonseparable potential in Eq. (15), a jump of

$$\mathbf{r}_{m,n} = m \left(\frac{a}{2}, -\frac{a}{2}, \frac{a}{2} \right) + n \left(-\frac{a}{2}, \frac{a}{2}, \frac{a}{2} \right)$$

goes over m saddle points along $\langle \bar{1}\bar{1}1 \rangle$ axis and n along $\langle \bar{1}11 \rangle$ axis. Plotted in Figs. 7 and 8 are the probability $\sum_n P(\mathbf{r}_{m,n})$ vs m extracted from the dynamic structure factor and the corresponding value obtained from the direct count-

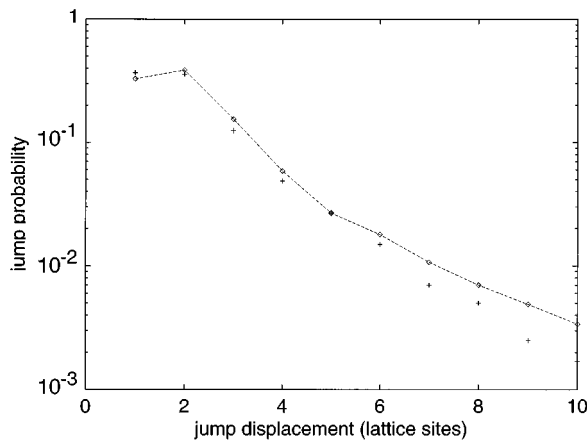


FIG. 7. Probability of jump as a function of distance projected along the $\langle \bar{1}11 \rangle$ direction for the nonseparable potential. Results are from direct jump counting based on the energy criterion (line with diamonds) vs that from the dynamic structure factor (crosses). $\Delta/k_B T=6.15$. Friction $\eta=0.01875\omega_0$.

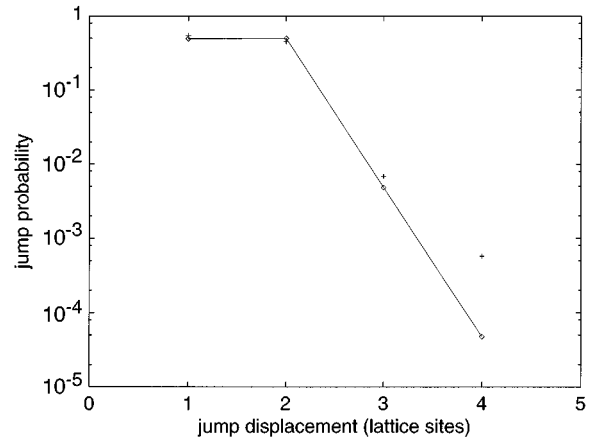


FIG. 8. Same as Fig. 7 except $\eta=0.15\omega_0$

ing data. Again, results from the two approaches agree well with each other. Moreover, in both the separable and the nonseparable cases, $\sum_n P(\mathbf{r}_{m,n}) = \sum_n P(\mathbf{r}_{n,m})$ as required by the surface symmetry. Comparing Fig. 8 with Fig. 6, for the same friction $\eta=0.15\omega_0$, we conclude that the probabilities of long jumps for the nonseparable potential are significantly less than those for the separable potential.

Now, we focus on the dependence of the long jumps on the value of friction. In Fig. 9, we plot the activation rate vs friction and, in Fig. 10, the mean square jumping displacements vs friction. These results are obtained for the nonseparable potential in Eq. (15) using the energy criterion for determining the end of a jump event. The activation rate (in some arbitrary units) can be evaluated by counting the total number of jumps of all lengths in a unit time interval. The temperature is chosen such that $\Delta/k_B T=6.15$. We find that the activation rate here has the same dependence on the friction as in the situation for the separable potential. The results in Fig. 9 show that the activation rate is proportional to the value of friction in the limit $\eta \rightarrow 0$. As the jump occurs over through saddle points at low temperatures, the mean square displacement along $\langle \bar{1}10 \rangle$ axis is twice of that along $\langle 001 \rangle$

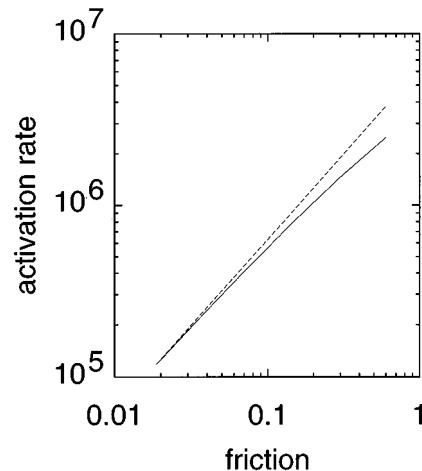


FIG. 9. Activation rate (arbitrary unit) vs friction η/ω_0 as obtained through MD simulation (solid curve). The dashed line is the linear behavior for comparison.

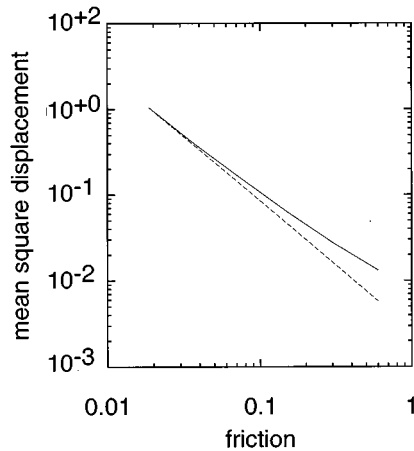


FIG. 10. Mean square jumping displacements (unit a^2) along (001) axis vs friction η/ω_0 (solid curve). The dashed line is the $1/\eta^{1.5}$ behavior for comparison.

axis as determined by the surface geometry. However, their dependence on the value of friction differ significantly from the separable potential case. Both mean square displacements are proportional to $1/\eta^{1+\alpha}$ ($\alpha \approx 0.5$) in the limit friction $\eta \rightarrow 0$. This is in direct contrast to the 1D or separable potential case where the mean square displacement assumes $\sim 1/\eta^2$ form. The dependence of the activation rate and the together leads to the result for the diffusion constant

$D \sim 1/\eta^{0.5}$ as discussed earlier. Thus we have confirmed explicitly our earlier assertions that the probability of the long jumps for the nonseparable 2D potential is different from the separable case because of the geometrical deactivation factor. The result that the mean square displacement should increase slower than the $1/\eta^2$ in the limit $\eta \rightarrow 0$ should be quite general for all nonseparable potentials. However, we expect the degree of the enhanced deactivation behavior to be sensitive to the shape of the potential, and hence the value of the exponent 0.5 in the behaviour $D \sim 1/\eta^{0.5}$ should not be universal.

In summary, we have presented a MD study of diffusion of a Brownian particle in two-dimensional periodic potentials. For a separable potential, our study recovers the results obtained through analytical approaches. For a nonseparable potential, our MD study yields new predictions on the friction dependence of diffusion constant in the low friction regime while it agrees with the existing literature in the intermediate to high friction regimes. Our MD study also predicts that the probability for long jumps depends sensitively on the surface geometry as well as on the value of the friction. We can make a general conclusion that compared with the results for a separable potential, the nonseparable adsorption potential leads to a reduction in the probability for long jumps and a weaker dependence of diffusion constant on the value of the friction in the low friction regime.

We thank Dr. P. L. Nash for helpful discussions. This work was supported in part by a grant from ONR.

¹V. I. Mel'nikov, Phys. Rep. **209**, 1 (1991).

²P. Hänggi, P. Talkner, and M. Borkovec, Rev. Mod. Phys. **62**, 251 (1990).

³R. Gomer, Rep. Prog. Phys. **53**, 917 (1990).

⁴H. A. Kramers, Physica **7**, 284 (1940).

⁵H. Risken, *The Fokker-Planck Equation* (Springer-Verlag, Berlin, 1989).

⁶R. Ferrando, R. Spadacini, and G. E. Tommei, Phys. Rev. E **48**, 2437 (1993).

⁷E. Pollak and P. Talkner, Phys. Rev. E **47**, 922 (1993).

⁸L. Y. Chen and S. C. Ying, Phys. Rev. Lett. **71**, 4361 (1993); Phys. Rev. B **49**, 13 838 (1994).

⁹S. C. Ying, Phys. Rev. B **41**, 7068 (1989); T. Ala-Nissila and

S. C. Ying, Prog. Surf. Sci. **39**, 227 (1992).

¹⁰E. Ganz, S. K. Theiss, I. S. Hwang, and J. Golovchenko, Phys. Rev. Lett. **68**, 1567 (1992).

¹¹D. C. Senft and G. Ehrlich, Phys. Rev. Lett. **74**, 294 (1995).

¹²V. P. Zhdanov, Surf. Sci. **214**, 289 (1989).

¹³K. Haug, G. Wahnström, and H. Metiu, J. Chem. Phys. **90**, 540 (1989); **92**, 2083 (1990).

¹⁴M. P. Allen and D. J. Tildesley, *Computer Simulation of Liquids* (Clarendon, Oxford, 1994).

¹⁵J. Ellis and J. P. Toennies, Phys. Rev. Lett. **70**, 2118 (1993).

¹⁶C. T. Chudley and R. J. Elliott, Proc. Phys. Soc. London **77**, 353 (1961).